SELF-FOCUSING EFFECTS IN COMPACT C-BAND STANDING-WAVE ACCELERATING STRUCTURE FOR X-RAY IMAGING APPLICATIONS*

H. R. Yang[#], S. H. Kim, S. J. Park, M. H. Cho, and W. Namkung
Pohang University of Science and Technology, Pohang 790-784, Korea
J. S. Oh
National Fusion Research Institute, Daejeon 305-333, Korea

Abstract

In electron RF linacs for industrial X-ray imaging applications, compact structures are preferred for mobility. The electron beam spot size of 1 – 2 mm is required for the spatial resolution of images at the X-ray conversion target. Applying self-focusing effects to the accelerating structure, external magnets can be removed and then the accelerator system becomes more compact. We design a C-band electron linac, which is capable of producing 6-MeV, 80-mA pulsed electron beams with an RF power of 1.5 MW. It uses a bi-periodic and on-axis-coupled accelerating structure with a built-in bunching section. It uses the π/2-mode standing-waves. The first bunching cell has an asymmetric geometry which maximizes the RF phase focusing. On the other hand, the normal cells are designed for the electrostatic focusing to be maximized. In this paper, we present design details of the accelerating cells and the beam dynamics simulation by the PARMELA code.

INTRODUCTION

There are growing demands on electron RF linacs for industrial radiographic applications such as the cargo inspection and non-destructive testing [1]. They require several MeV electrons for the bremsstrahlung radiation. Although lots of commercial products use the S-band RF, the C- and X-band RF is recently preferred for mobile systems. These applications require the beam spot size of 1 – 2 mm at the X-ray conversion target for the spatial resolution of X-ray images [2]. As the electron beams are focused by only RF not external magnets, the accelerator system becomes more compact since RF structures of C- and X-band are comparatively small.

We are developing an electron linac for industrial X-ray imaging applications. It is capable of producing 6-MeV electron beams with a pulsed beam current of 80 mA, which is powered by a pulsed 1.5-MW C-band magnetron. For beam energy and the accelerating gradient in the given input RF power, self-focusing effects can be appeared in the accelerating structure. We evaluate the focusing strength by each effect and design details of bunching and normal cells of the accelerating structure. These are optimized for the self-focusing effects. We also investigated beam dynamics simulations with PARMELA codes.

_____

SELF-FOCUSING EFFECTS

The self-focusing effects are distinguished by origins of the focusing fields: the electrostatic focusing, the RF phase focusing, and the ponderomotive focusing. The electrostatic focusing occurs in an accelerating gap with static electric fields. The radial force is represented by [3]

$$F_r = -\frac{e^2 r}{4\beta\gamma mc^2}\left(<E^2> - <E>^2\right), \qquad (1)$$

where, e is the electron charge, r is the radial position, β is the particle speed of over c, γ is the relativistic factor, m is the particle mass, and E is the amplitude of the electric field.

In RF accelerating cavities, the particle experiences radial forces asymmetric to the middle of the cavity, since the electric fields vary in time. The net radial impact depends on the injection phase into the cavity. This effect is called a RF phase focusing and the radial force is represented by [4]

$$F_r = -\frac{er}{2}\frac{k}{\beta\gamma^2}E_z \sin\varphi , \qquad (2)$$

where, k is the wave number and φ is the particle phase relative to the reference particle on the wave crest. For electrons, the particles followed by the reference particle ($\varphi < 0$) are focused, while the particle following the reference particle ($\varphi > 0$) are defocused.

For electron beams in an accelerating cavity with E_0 of 12 MV/m at φ of 10°, those two effects are calculated with beam energies. In Fig. 1, the focusing strength $1/f$ is defined by [5]

$$\frac{1}{f} = -\frac{F_r}{r\beta^2\gamma mc^2}\cdot l , \qquad (3)$$

where, l is the longitudinal length of the accelerating cavity. Since the RF phase focusing is dominant in the lower energy region, the bunching cells should be designed to maximize this effect. On the other hand, the normal cells should be designed for the ponderomotive focusing to be maximized. However, in general, the beams are de-bunched in the focusing phase by the RF phase focusing. Therefore, a configuration of the

bunching cells should be selected carefully for the beam focusing as well as the beam bunching.

Even though the electrostatic focusing is small in the high energy region, the beam size can be effectively reduced with higher accelerating gradients as shown in Fig. 2. The radial field in Eq. (1) is proportional to squares of the electric fields. Since the input RF power is limited by the 1.5-MW C-band magnetron, and the beam energy should be 6 MeV, a reasonable accelerating gradient is 12 MV/m. At this accelerating gradient, the beam focusing is achieved by a configuration of the bunching cells and an adjustment of the cell geometries.
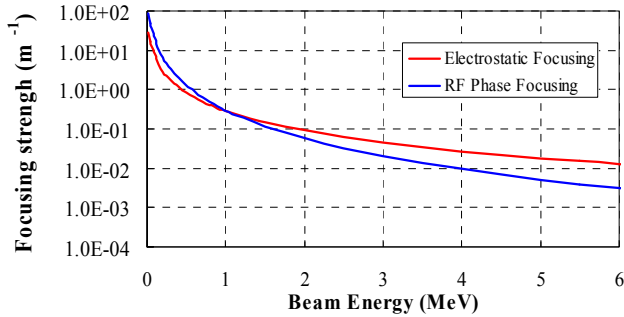

Figure 1: The variation of the self-focusing effects by the variation of the particle energy. The effects are calculated in one cell with E_0 = 12 MV/m, φ = 10°.
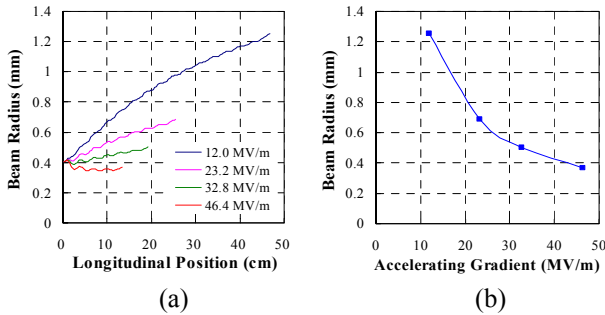

Figure 2: The beam radii with accelerating gradients. The values are obtained by the PARMELA simulation. The initial beam energy is 1 MeV and accelerated up to 6 MeV. The initial emittance is 20 mm-mrad with a bunch length of 30°, (a) the beam envelope along the accelerating structure and (b) the beam radius at the end of the structure.

BUNCHING CELL

The first bunching cell has an asymmetric geometry to the middle of the cavity. The particle in the focusing phase experiences the higher accelerating field than the one in the defocusing phase [4]. Adopting the asymmetric first bunching cell, the beam radius is reduced as shown in Fig. 3. For the cell-A, the field profile is almost symmetric as shown in Fig. 3 (a) while the field profile of the cell-B is asymmetric as shown in Fig. 3 (b). As we change the first bunching cell from the cell-A to the cell-

B, the final beam radius is reduced by about 30%, as shown in Fig. 3 (c). The phase velocity of the first bunching cell is 0.3 c. The results in Fig. 3 (c) are calculated by the PARMELA code with initially 20-keV DC beams. The input beam current is 150 mA and the transmission rate is 60%.

The injection phase into the normal cells affects on the beam transmission and average beam energy as well as the beam focusing. The injection phase in Fig. 4 is determined as 40° in order to achieve the beam size less than 1.3 mm, while the beam energy is more than 6 MeV and the beam transmission rate is more than 60%. For that injection phase, the phase velocities of the rest bunching cells are selected as 0.3, 0.5, and 0.9 c, respectively.
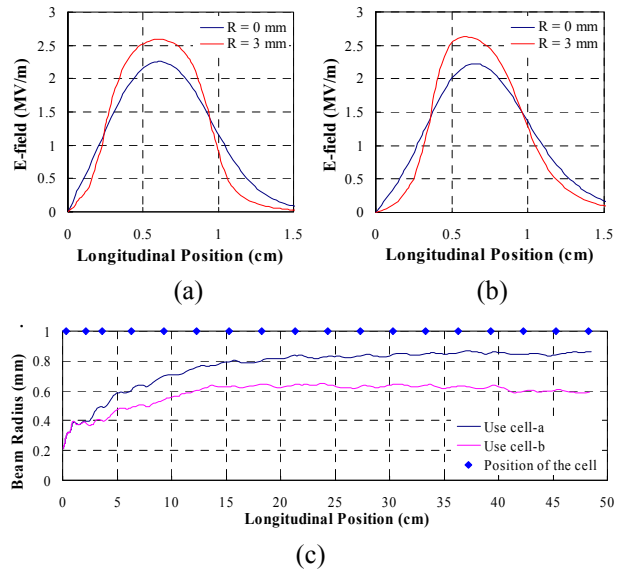

Figure 3: On-axis electric fields along the first bunching cell for (a) cell-A and (b) cell-B. The beam envelopes in (c) are calculated for these two cases.
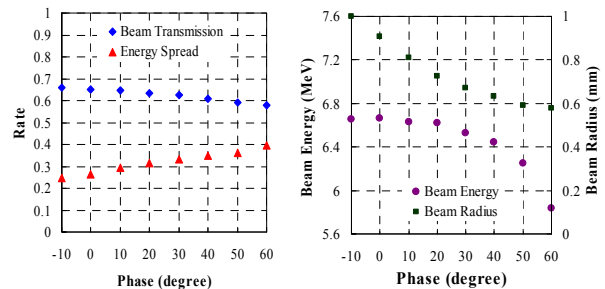

Figure 4: The variation of the output beam parameters by the variation of the injecting beam phase in the normal section. The result is obtained by the PARMELA simulation with 20-keV, pulsed 150-mA input beam.

NORMAL CELL

The normal cell with a nose-cone shape is identified by geometric parameters as shown in Fig. 5: the gap size L, the iris radius a, the width of the coupling cell D, and the

curvature radius R. a is set to be 4 mm for the safe beam transmission. D is set to be 2 mm considering machining tolerances. L affects on both the electrostatic and RF phase focusing. As L becomes smaller, the radial force by the electrostatic focusing increases according to Eq. (1). On the other hand, RF focusing effect is reduced since the effective shunt impedance decreases. The gap size is determined as 15 mm compromising those effects, as shown in Fig. 6. The curvature radius is determined as 12 mm in order to maximize the effective shunt impedance
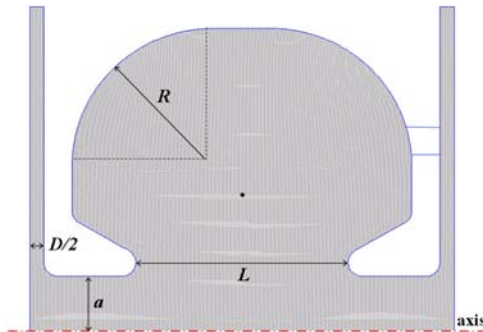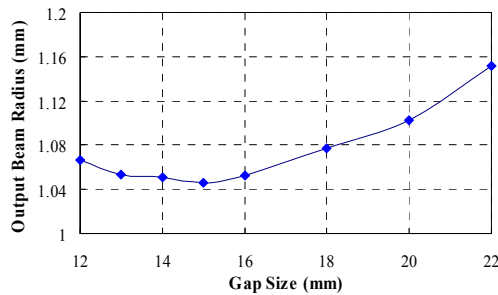

Figure 5: Geometry of the normal cell.

Figure 6: Output beam radius with gap sizes calculated by PARMELA code. The initial beam parameters and bunching cells are the same to that in Fig. 2.

SUMMARY

The C-band accelerating structure is designed. It is capable of producing 6-MeV, 80-mA pulsed electron beams with an RF power of 1.5 MW. In order to remove external magnet from the accelerator system, the RF phase focusing is applied to the bunching cells, especially the first bunching cell which has the asymmetric geometry, while the electrostatic focusing is applied the normal cells. The beam radius is less than 1.3 mm when the beam energy is 6 MeV, according to the simulation results by the PARMELA code. The detailed accelerator parameters are listed in Table 1.

Table 1: The parameters of the accelerating column

Operating Frequency	5 GHz
Input Pulsed RF Power	1.5 MW
E-gun Voltage	20 kV
Input Pulsed Beam Current	150 mA
Output Beam Energy	6 MeV
Output Pulsed Beam Current	80 mA
Type of Structure	Bi-periodic, On-axis coupled
Operating Mode	SW π/2 mode
Beam Aperture Diameter	8 mm
Average Accelerating Gradient	13.81 MV/m
Number of Cells	17
Quality Factor[*]	12000
Effective Shunt Impedance[*]	100 MΩ/m
Transit-time Factor[*]	0.84

[*]Values for normal cells.

REFERENCES

[1] C. Tang, et al, "Present Status of the Accelerator Industry in Asia," in *Proc. of IPAC10* (Kyoto, Japan, May 23-28, 2010), p. 2447.

[2] C. Hao, et al, "A New Type SW Linac Used in Industrial CT," in *Proc. of APAC 2004* (Gyeongju, Korea, March 22-26, 2004), p. 429.

[3] R. H. Miller, H. Deruyter, W. R. Fowkes, J. M. Potter, R. G. Schonberg, and J. M. Weaver, IEEE Trans. Nucl. Sci. **NS-32**, No. 5, 3231 (1985).

[4] S. Xiang, et al, "RF Phase Focusing and Asymmetric Field Shape in Standing-wave Electron Linacs," in *Proc. of APAC98* (Tsukuba, Japan, Mar. 23-27, 1998).

[5] S. H. Hartman and J. B. Rosenzweig, Phys. Rev. E **47**, No. 3, 2031 (1993).